Microreactors technology for hydrogen purification: Effect of the catalytic layer thickness on CuO_x/CeO_2-coated microchannel reactors for the PROX reaction

O.H. Laguna*, M. González Castaño, M.A. Centeno, J.A. Odriozola

Instituto de Ciencia de Materiales de Sevilla, Centro Mixto CSIC – Universidad de Sevilla, Avenida Américo Vespucio 49, 41092 Seville, Spain

*Corresponding author e-mail: ohlaguna@icmse.csic.es

Keywords

Microreactor; Process intensification; CO-PROX; Catalytic layer thickness

Abstract

Two blocks of microreactors composed by 100 microchannels and coated, respectively, with 150 and 300 mg of a CuO_x/CeO_2 catalyst, were prepared and tested in the preferential oxidation of CO in presence of H_2 (PROX). The deposition of different amount of catalyst resulted in different catalytic layer thicknesses thus modifying the catalytic performances of the microreactor. The evaluation of the main reaction variables (the space velocity, the O_2-to-CO ratio and the presence of H_2O and/or CO_2 in the stream) was performed over both microreactors and compared to that of the parent powder catalyst. The least loaded microreactor, with a coating thickness around 10 μm, presented the highest CO conversion and selectivity levels at temperatures below 160 ºC. This result evidences i) the improvement of the catalytic performances got by the structuration of the powder catalyst and ii) the importance of the selection of the adequate thickness of the catalytic layer on the microreactor, which have not to exceed and optimal value. An adequate coating thickness allows minimizing the mass and heat transport limitations, thus resulting in the enhancement of the catalytic performance during the PROX reaction.

1. Introduction

Currently, the need for alternative energy sources motives the development of new technologies based on fuels different to those based in petroleum. In this sense, many efforts have been focused in the use of H_2 for transport and portable applications [1, 2]. However the production of H_2 is a multi-stage process including reforming of hydrogen-containing fuels, such as hydrocarbons and alcohols, followed by successive cleaning up steps for up-taking the CO, such us the high and low temperature water-gas-shift (HT and LT-WGS) and the preferential oxidation of CO (PROX). These processes should reduce the CO levels around 1% in the case of the WGS, and then below 50 ppm with the PROX, in order to ensure a longer lifetime of the electrochemical devices where the H_2 fuelled is converted in electric power. In this sense, highly active catalysts in the CO abatement reactions are required. Actually many systems with different supports and active phases have been tested in CO oxidations reactions [2-7].

The real application of the H_2 technology in automotive and portable devices strongly depends on the incorporation of the different reactions involved into the engine of these systems. Besides this, the size of the compact fuel processors where the different reactions occur must be adequate for the efficiency during the transport [1]. In this regard, the microreactors are an interesting option if their diverse advantages are considered [8, 9]. The microreactors can be considered as small scale chemical reactors that achieve high conversion rates within a reduced volume [10, 11]. These devices allow the process intensification because they are able to enhance the heating exchange, being especially attractive for exothermic reactions where a strict temperature control has to be achieved. Moreover, the total flow of the feeding and the pressure in the inlet can be considerably increased, compared with those of the common packed-bed reactors. In addition, a more direct transition from the laboratory to the industrial production scale is easily achievable for microreactors [8, 9].

Several works have presented interesting progresses on the application of microreactors in different reactions [12, 13]. For example, Jang et al. [14]

studied a micro-methanol steam reformer and established that the geometry of the manifold and the channel size, among other variables, had a crucial influence on the efficiency and consequently must be optimized for every microreactor. This agrees with the results presented by Mathieu-Potvin et al. [10] that analysed, by a numerical simulation study, the optimal geometry of catalytic microreactors. They conclude that the competition between diffusion, advection and kinetic phenomena dictate the design of the microreactors. In this sense, some adimensional numbers must be considered, such us the Schmidt and the Bejan number that are related to the behaviour of the fluid into the channels. Additionally, it was pointed out that the simulation of the microreactor behaviour requires the optimization of the mass of catalyst introduced into the microchannels and of the total flow used, in order to achieve the adequate aspect ratio that improves the maximum conversion.

Among the different variables considered during the designing and manufacturing of microreactors, the optimization of the amount of loaded catalyst is a capital parameter for obtaining the maximum catalytic performance and consequently, the control of the catalytic layer thickness results determinant. This variable may strongly influence the heat and mass transport phenomena on the catalytic behaviour of the microreactor. In this sense, the modification of the products distribution by the variation of the selectivity and the decreasing of the heat transport could be noticeable if the catalytic layer thickness is outside the optimal value.

The efficient releasing of heat during the reaction is crucial for exothermic processes such as PROX. Microreactors may improve the releasing of the heat produced in such exothermal reactions avoiding the formation of hot spots and allowing a strict control of the reaction temperature. For instance, recently Llorca et al. [15] have presented the study of a silicon micromonolith containing ca. 40000 regular channels of 3.3 μm in diameter per square millimeter containing Au/TiO_2 as the catalysts coated in the walls of the channels, for the PROX reaction. The authors demonstrated that although their silicon microreactor did not achieve high CO conversions levels at low temperatures (150 – 240 ºC), this system was considerably more efficient than a conventional

400 cpsi (cells per square inch) cordierite monoliths, which presented a poor heat transfer during the process.

Ouyang et al. [16] have showed the lower radial and axial temperature gradients in microreactors compared to those of packed bed reactors, which minimize the extend of the reverse WGS reaction, and favour higher CO conversions. However, if the amount of catalyst coated in the walls of the microchannels is very high, this better heat releasing rate may be less obvious, and the occurrence of some mass transport limitations inside the catalytic layer cannot be fully discarded. This problem was studied by Potemkin et al. [17] over a microreactor loaded with a 5 wt.% Cu/CeO_{2-X} catalyst. The authors proposed the calculation of an internal effectiveness factor (η_{CO}), determined as the ratio of the reaction rate calculated assuming the existence of mass transfer limitations to that calculated in the assumption of zero mass transfer limitations. The analysis of the η_{CO} factor for different thickness of catalytic layers suggested that the lowest contribution of mass transport limitations in microreactors is produced when the thickness does not exceed ~20 μm. Obviously, we must take into account that this value is approximate and only valid for the specific catalyst used in that work, since the textural properties of the catalyst (pore size distribution, etc.) may control the kind and rate of diffusion of the reagents and products along the channels.

From all above, it is clear that the development of microreactors still requires additional studies where many variables have to be optimized in order to generate a complete knowledge about the designing, manufacturing and applying of microreactors as catalytic systems. The present work pretends to analyse different catalytic experimental results obtained with two blocks of microreactors, composed by 100 microchannels, coated with different total amounts of a $CuOx/CeO_2$ catalyst (150 and 300 mg) for the PROX reaction.

2. Materials and methods

2.1. Synthesis of the CuO_x/CeO_2 catalyst and manufacturing of the microreactors

Recently we have published the experimental procedures for the synthesis and the characterization by means of N_2 adsorption-desorption, XRD, Raman spectroscopy and H_2-TPR studies of the CuO_x/CeO_2 powder catalyst [18, 19]. The manufacturing process of our microreactor prototype coated with 300 mg of catalyst [4, 18-20] is summarized in Figure 1. In the present work, this microreactor is named as MR300 and will be compared with a new block coated with 150 mg of catalyst, denoted as MR150.

2.2. Catalytic activity measurements

Prior to every catalytic test the catalysts were treated under 30 mL/min total flow of 21% O_2 in N_2 at 300 ºC for 2 h. For the powder catalyst, the PROX reaction was carried out in a fixed-bed cylindrical stainless steel reactor with internal diameter of 9 mm under the experimental conditions presented in [21]. For these experiments, 100 mg of catalyst (particle size= $100 < \phi < 200$ μm) were employed and diluted with crushed glass (in the same particle size) forming a bed of about 50 mm in length. The CO conversion and the selectivity to CO conversion were calculated according to Eq. 1 and Eq. 2, respectively. F_{in} and F_{out} refer to molar flow rates at the reactor inlet and outlet, respectively [4, 20].

$$\text{CO conversion (\%)} = \frac{(F_{CO,in} - F_{CO,out}) \times 100}{F_{CO,in}} \qquad \text{(Eq.1)}$$

$$\text{Selectivity to CO conversion (\%)} = \frac{(F_{CO,in} - F_{CO,out}) \times 100}{2(F_{O_2,in} - F_{O_2,out})} \qquad \text{(Eq.2)}$$

In the case of microreactors, the same reaction set-up was used; however the cylindrical reactor was replaced by two stainless steel cases connecting the inlet and outlet positions of the microchannels, and allowing the contact between the coated walls of the channels and the feed-stream according to that described in [4, 20]. The temperature was continuously monitored by 4 K-type thermocouples. Two of them were placed in contact with the metallic block at

the inlet and outlet positions of some central microchannels. The other two sensors recorded the temperature at lateral positions in the walls of the microreactor [4]. The feed-stream compositions and the λ values used in the catalytic tests are presented in Table 1. The λ value was calculated for every mixture of reaction according to Eq. 3 [22].

$$\lambda = \frac{[2 \times O_2 vol.\%]}{CO vol.\%} \quad \text{(Eq. 3)}$$

A first comparison of the catalytic performances of the three catalysts studied, the powder and the MR150 and MR300 microreactors, was carried out employing the feed-stream A and maintaining the flow-to-catalyst weight ratio in 60 $L \cdot h^{-1} \cdot g^{-1}$. Additionally, the influence of the space velocity (30, 60 and 120 $L \cdot h^{-1} \cdot g^{-1}$) was analyzed for both microreactors applying the feed-stream B. The influence of the λ value was also evaluated by using the feed-streams B, C and D at a constant space velocity of 60 $L \cdot h^{-1} \cdot g^{-1}$. Finally, the effect of the presence of CO_2 and/or H_2O was studied with the feed-stream compositions A, E, F, and G at a constant space velocity of 60 $L \cdot h^{-1} \cdot g^{-1}$.

3. Results and discussion

3.1. Comparison of the CuO_x/CeO_2 powder catalyst and the microreactors MR150 and MR300 for the PROX reaction

The catalytic results obtained for the CuO_x/CeO_2 powder catalyst and for the two microreactors under a space velocity of 60 $L \cdot h^{-1} \cdot g^{-1}$ are presented in Figure 2.

In all three catalysts, the CO conversion increases with temperature near to full conversion at 160ºC and above (Figure 2A). However at temperatures below 160 ºC, different behaviours are appreciable. MR150 presents the highest

catalytic activity while the MR300 exhibits the lowest CO conversion levels. The powder catalyst presents an intermediate behaviour.

The selectivity to CO conversion (Figure 2B) decreases with the temperature in the three cases. Both microreactors present similar selectivities each other but higher than that of the powder catalyst, which suggests that the H_2 consumption reactions (H_2 oxidation and/or R-WGS) would be inhibited in them.

From here, it is clear that the microreactor loaded with the lowest amount of catalyst (MR150) presents better catalytic performances than those of the powder catalyst. Besides this, although both microreactors has a similar selectivity to CO_2, the highest CO conversion levels showed by the lowest loaded microreactor (MR150), makes it the system with the best performance.

The observed differences in CO conversion and selectivity among the three evaluated systems may be attributed to the existence and different extension of mass and heat transport phenomena. The highest catalytic activity of the MR150 microreactor, must be related with the best efficiency in the release of the heat produced by the exothermic reactions implied (CO and H_2 oxidations and WGS). This allows a better thermal control into the microchannels and ensures the isothermal conditions at every evaluated temperature, avoiding the hot spots formation. Consequently, although the difference between the apparent activation energies for the CO and H_2 oxidation reactions is not so big (36.9 and 110 kJ/mol respectively) [21], the achieved strict control of the temperature in the MR150 delays the appearance of the H_2 oxidation reaction, especially at lower temperatures. Our results are in good agreement with the highly efficient heat transfer that has been widely described for other microreactors employed in the PROX reaction, some of them coated with CuO_x/CeO_2 catalysts [16, 23, 24]. For instance Snytnikov et al. [25] have studied a copper-cerium oxide catalyst for the PROX reaction as a powder catalyst in a fixed-bed reactor and coated in microreactors. They have proposed that in the case of microreactors, the releasing of the heat produced during the oxidation reaction is very fast because of the direct contact between the catalytic layer and the metal substrate. However, in the case of the fixed-bed

reactor, the presence of quartz, which is used as diluent, may present heat transport limitations due to its rather low thermal conductivity. A similar effect could occur in our case for the powder catalysts, since it was tested in a fixed-bed reactor and diluted with ground glass.

Besides this, the superior catalytic behaviour of the MR150 microreactor respect to that of the powder catalyst may be also associated to the diminution of the mass transfer limitations in the structured systems. Probably, the contact between the catalyst and the reaction mixture is different in both situations and, additionally, the presence of ground glass with the powder catalyst in the fixed-bed reactor also represents an additional barrier for the adequate mass transport.

Despite the advantage of the MR150 structured system, the lower catalytic performance at temperatures below 160ºC of the MR300, even inferior to that of the powder catalyst highlights the need to optimize the amount of coated catalyst in the microreactors, that consequently means the need to optimize the thickness of the catalytic layer. As said in the introduction section, the relevance of optimizing of the catalytic layer thickness was emphasized by Potemkin et al. [17] who demonstrated that that optimum values of the internal effectiveness factor for the CO oxidation, η_{CO}, which assures no mass limitations, for the PROX reaction over a microreactor coated with a Cu/CeO_{2-x} catalyst in the 170–230ºC temperature range, are achieved when the washcoated thickness did not exceed 20 μm.

3.2. Effect of the space velocity over the microreactors

In order to evaluate the influence of the space velocity on the catalytic performances of the structured systems, three total flow to weight of catalyst ratios were studied (30, 60 and 120 $L \cdot h^{-1} \cdot g^{-1}$), keeping the same composition of the reactive feed and with a $\lambda = 1$ value. The results of CO conversion and selectivity to CO oxidation are presented in Figure 3.

The MR150 microreactor presents a maximum in the CO conversion at around 140 ºC whatever the space velocity used, although the value of such maximum conversion decreased when increasing the space velocity. Moreover, higher the space velocity of the experiment, lower the catalytic activity of the system at temperatures below 140 ºC. On the other hand, the MR300 microreactor shows a remarkable increasing of the CO conversion with the temperature, no matter the space velocity, up to 160 ºC. At higher temperatures, the catalytic activity tends to stabilize. In every case, the conversion curves shift to higher temperatures when increasing the space velocity.

The block coated with 300 mg of catalyst exhibits higher conversions than those of the MR150 microreactor at high temperatures. However, in this temperature range, the MR150 preserves a superior selectivity to CO oxidation. For both microreactors, the increment of the space velocity results in the decrease of the catalytic activity, especially at temperatures below 160 ºC. Considering that maldistributions of feed-stream into the channels of the studied microchannels blocks may be discarded according to previous CFD studies carried out for designing the microreactors and the cases for inserting them in the reaction system [26], the low CO conversion shown by both blocks, especially at low temperatures occurs because the active sites are working under demanding conditions (a high amount of CO molecules to be converted per unit of time and an insufficient thermal activation), showing their full potential. Snytnikov et al. [23] reported similar observations studying microreactors coated with Cu/CeO_{2-x} for the PROX reaction. They concluded that, when the flow rate is increased, the minimum outlet CO concentration is increased and the optimum reactor working temperature, corresponding to the minimum CO concentration emission, was shifted to higher values.

Concerning the selectivity to CO oxidation (Figure 3B), a general view allows establishing that the MR150 microreactor presents higher selectivities than those of MR300 in all cases, especially at temperatures above 160 ºC. However, the modification of the space velocity seems to produce an opposite effect in every microreactor. In the case of the MR150, when the space velocity is increased, the selectivity also increased. However, for the MR300

microreactor, no big differences are observed for the space velocities of 30 and 60 $L \cdot h^{-1} \cdot g^{-1}$, but a loss of selectivity is detected for 120 $L \cdot h^{-1} \cdot g^{-1}$.

A similar behaviour of the selectivities increasing with the space velocity for the MR150 was observed by Roberts et al. [27] in their study about Pt/Fe monolithic catalysts for the PROX reaction. They established that the CO selectivity increased with increasing the space velocity while the CO and O_2 conversions decreased and proposed that the R-WGS reaction was more important at low space velocities. However, these authors also have associated the transport effects to the behaviour of their structured catalyst, because the possible decreasing of the catalytic performance by reducing "the contact time" (higher space velocities) was partially off-set by increasing the heat and mass transfer coefficients. This would explain the differences between the MR150 and MR300 blocks, being the most loaded microreactor influenced not only by the R-WGS but also by low heat and mass transfer speed.

3.3. Effect of the O_2/CO molar ratio (λ) over the microreactors

The CO conversion and the selectivity to the CO conversion for both analysed microreactors as a function of the O_2/CO ratio in the feed-stream are presented in Figure 4.

The CO conversion for the MR300 microreactor (Figure 4A) increased with temperature until values close to 100%, no matter the applied λ value. Nevertheless, below 160 ºC a sequence of activity as a function of λ is observed: λ = 2.0 > λ = 3.0 > λ = 1.5. On the contrary, the MR150 microreactor did not present large differences in the conversion curves obtained as a function of λ, which agrees with all discussed above concerning the lower heat and mass transport limitations presented in this microreactor. This characteristic results in a more active system whose catalytic activity is not strongly influenced by the amount of oxygen present in the feed.

In all experiments, the selectivity to CO oxidation decreased with the temperature (Figure 4B). However, the modification of the amount of O_2 in the

feed-stream had a stronger effect for the MR150 microreactor. For λ = 2, this microreactor showed the highest selectivity at temperatures below 180 ºC. The catalytic results showed in figure 4 evidence that the variation in the λ values produces changes only in the selectivity to CO oxidation in the case of the microreactor with the smaller catalytic layer thickness (MR150). However, for the high loaded microreactor (MR300) modifications of both, the CO conversion and selectivity are observed as a function of λ.

Again, these results agree with those presented in the other sections of this paper, and can be related with the improvement of the mass and heat transfer phenomena in the microreactor with the smallest catalytic layer thickness (MR150). Thus, as a general rule, it is obvious that the improvement of heat transport phenomenon and the successful isothermal control achieved during the PROX reaction seems to be a relevant contribution of microreactors. Besides this, the mass transport limitation must be also considered. Concerning this regard, it is very difficult to quantify which is the individual contribution of each phenomenon (heat and mass transport limitations) in the observed catalytic behaviour, because both occur simultaneously.

Despite this, we have considered the methodology proposed by Weisz and Hicks for estimating the effectiveness factors in catalytic processes with internal mass and heat diffusion effects [28] and some assumptions must be accounted. Taking into account the excess of H_2 in the feed-stream, and the small size of the H_2 molecule, an effectiveness factor ηH_2 =1 may be assumed under typical PROX conditions (implying an excess of this compound) [17]. But in the case of CO, the effectiveness factor (ηCO) is different for the powder catalyst, the MR150 and the MR300 microreactors. The ηCO values were then estimated in terms of observable parameters strategy proposed in [28], calculating the parameters ϕ, γ, and β according to Eqs. 4-6 .

$$\phi = \frac{dN}{dt}\frac{1}{C_0}\frac{R^2}{D} \qquad \text{Eq.4}$$

$$\gamma = \frac{Ea}{RT_0} \qquad \text{Eq. 5}$$

$$\beta = \frac{C_0 HD}{KT_0} \quad \text{Eq. 6}$$

In Eq. 4, *dN/dt* represents the rate of reaction, therefore the kinetic parameters and the rate expressions obtained in the kinetic study of the CuO_x/CeO_2 catalyst are employed. C_0 is the CO concentration and D is the effective diffusivity, calculated for the CuO_x/CeO_2 catalyst according to that proposed by Potemkin et al. [17], considering the molecular and Knudsen diffusion. R is the radii of the particle in the case of assuming spherical geometry for the catalyst. In the case of the powder catalyst an average diameter of 150 μm was assumed. As for the MR150 and MR300, the catalytic layer thickness was transformed into the diameter of the equivalent spherical particle according to Almeida et al. [29], obtaining 30 μm for MR150 and 60 μm for MR300. On the other hand, in Eq. 5, *Ea* represents the activation energy for the CO oxidation reaction and T_0 is the temperature. Finally, in Eq. 6, *H* represents the enthalpy of reaction of the CO oxidation and *K* is the thermal conductivity. For this last parameter, a typical value for non-metallic solids with a relatively narrow pore-size distribution, which is the case of the CuO_x/CeO_2 solid [28], was employed ($K = 5x10^{-4}$ cal/[cm x s x ºK].

Once the ϕ, γ, and β parameters were calculated at the different temperatures evaluated during the catalytic tests for the three studied systems presented in Figure 1 (Feed-stream A – see Table 1), the effectiveness factor (ηCO) could be interpolated in the functional dependence of utilization factor of observable quantities, reported by Weisz and Hicks and the results are presented in Figure 6.

Despite the assumptions that must be considered for calculating the effectiveness factor for CO, the results presented in Figure 6 demonstrated the contribution of internal mass transport limitations principally for the powder catalyst. Concerning the microreactors, some internal mass transfer limitation is

detected with increasing the temperature. Especially the MR300 presented a superior catalytic layer thickness. These observations demonstrated that the catalytic performance during the PROX reaction is not only driven by the heating exchange for ensuring an adequate thermal control but also depends on the contribution of the mass transport phenomena. Particularly in the case of the microreactors, the catalytic layer thickness must be optimized in order to minimize the transport limitations. It must be remarked that the MR150 system showed ηCO values practically equal to 1 for all the studied temperatures. This indicated that for the design of microreactor evaluated in this study, the catalytic layer obtained with the loading of 150 mg of CuO_x/CeO_2 catalyst seems to be close to the optimal value, in order to minimize the heat and mass transport limitations.

Despite the similar behaviour described in the present work and that published by Potemkim et al [17] concerning the existence of an optimal thickness of the catalytic layer deposited on microreactors, and considering the applying of a relatively similar catalyst, the optimal layer thickness is not the same in both works. These authors have proposed an optimum coating thickness of 20 μm. In our case, assuming a perfect and homogeneous coating by the catalyst on the MR150 and MR300 microreactors, the calculated thicknesses are 10 μm and 19 μm respectively. These values were obtained from the estimation of the volume of the coating. For this purpose, the total area of the microchannels (60 cm^2), the total mass of every coverage (150 and 300 mg), the pores volume of the dried (0.213 cm^3/g) slurry and the apparent density of the deposited solid (5.9 g/cm^3) [30] were considered.

Although there are optimal conditions where the best performance in the PROX reaction is obtained for microreactores, other aspects such as the design and material of the block, the size and shape of the channels, and most likely the nature of the catalyst, must be also considering for the tuning of the reaction setup. Moreover a scale factor must be also taken into account for the optimization of a catalytic device for the PROX reaction because, for example the microreactors employed by Potemkin et al. [17, 25], with 14 microchannels, exhibit an optimal performance for catalytic layers around 20 μm, while in our

prototype with 100 microchannels, the catalytic layer with 19 μm presents heat and mass transport problems, while the microreactor with a catalytic layer around 10 μm exhibits a better catalytic performance.

3.4. Effect of H_2O or/and CO_2 in the feed-stream over the microreactors

The presence of H_2O and CO_2 in the feed-stream during the PROX reaction has been evaluated together and separately for the MR150 and MR300 systems. The catalytic activity results are presented in Figure 5.

Similarly to the behaviour described in previous sections when changing others reaction parameters (space velocity, reactant composition and λ value), the influence of the CO_2 and/or H_2O presence in the feed is markedly different from both microreactors. In the case of the least loaded one (MR150), no significant alterations are observed in the catalytic curves, and a wide operation window from 130 to 180 ºC where the maximum CO conversion occurs, is observed in all cases. Only, a loss of activity is detected at low temperatures in the experiments carried out with CO_2. This agrees with the well reported deactivation phenomena occurring in the surface of the catalysts by the adsorption/reaction with gaseous CO_2, forming carbonaceous species that blocks the active centres, which is more evident at low temperatures [30]. On the other hand, this results points out that the incorporation of CO_2 in the feed-stream may drive the equilibrium towards the R-WGS. In the case of the highest loaded microreactor, MR300, a combination of the poor heat and mass transport respect to that of the MR150 one is suggested with the promotion of the R-WGS reaction by the inclusion of CO_2.

4. Conclusions

Two microreactors composed by 100 microchannels and coated with 150 and 300 mg of a CuO_x/CeO_2 catalyst have been successfully evaluated under different experimental conditions for the PROX reaction. The least loaded microreactor (MR150) shows a higher catalytic activity (CO conversion belong to high selectivity) compared to those of the microreactor coated with 300 mg

and the powder catalyst (MR300). The better catalytic performance of the MR150 (with an ideal catalytic layer thickness around 10 μm) is directly associated to the enhancement of the heat transport, which allows an optimal thermal control of the reaction. This results in the enhancement of the catalytic activity at low temperature (< 160 ºC) and providing resistance to the microreactor to the changes of the O_2/CO ratio in the feed-stream. Additionally for this microreactor, the resistance to the loss of activity at low temperatures by the presence of H_2O and/or CO_2, compared with that of the MR300 one, allows establishing that the structuration of the catalyst with the adequate amount of catalyst also enhances the mass transport during the PROX reaction.

5. Acknowledgements

The authors thank the financial support from the Ministerio de Economía y Competitividad Español (ENE2012-374301-C03-01 and ENE2013-47880-C3-2-R) being co-financed by FEDER funds from the European Union and from Junta de Andalucía (TEP-8196). In addition the authors thank to Dr. Juan Almagro (ACERINOX S.A. Spain) for his help with high-resolution FESEM experiments.

6. References

[1] G. Kolb, Fuel Processing for Fuel Cells, Wiley-VCH Verlan GmbH & Co. KGaA, Weinheim, 2008.

[2] R.J. Farrauto, Chemical Engineering Journal, 238 (2014) 172-177.

[3] K.Y. Ho, K.L. Yeung, Gold Bulletin, 40 (2007) 15-30.

[4] O.H. Laguna, M.I. Domínguez, S. Oraá, A. Navajas, G. Arzamendi, L.M. Gandía, M.A. Centeno, M. Montes, J.A. Odriozola, Catal. Today, 203 (2013) 182-187.

[5] X. Li, H. Dai, J. Deng, Y. Liu, S. Xie, Z. Zhao, Y. Wang, G. Guo, H. Arandiyan, Chem. Eng. J, 228 (2013) 965-975.

[6] J.L. Ayastuy, A. Iglesias-González, M.A. Gutiérrez-Ortiz, Chemical Engineering Journal, 244 (2014) 372-381.

[7] P.-Y. Peng, I. Jin, T.C.K. Yang, C.-M. Huang, Chemical Engineering Journal, 251 (2014) 228-235.

[8] K. Jahnisch, V. Hessel, H. Lowe, M. Baerns, Angew. Chem.-Int. Edit., 43 (2004) 406-446.

[9] G. Kolb, Chem. Eng. Process., 65 (2013) 1-44.

[10] F. Mathieu-Potvin, L. Gosselin, A.K. Da Silva, Chemical Engineering Science, 73 (2012) 249-260.

[11] W.N. Lau, K.L. Yeung, R. Martin-Aranda, Microporous and Mesoporous Materials, 115 (2008) 156-163.

[12] G. Chen, Q. Yuan, H. Li, S. Li, Chemical Engineering Journal, 101 (2004) 101-106.

[13] S. Tadepalli, R. Halder, A. Lawal, Chemical Engineering Science, 62 (2007) 2663-2678.

[14] J.Y. Jang, Y.X. Huang, C.H. Cheng, Chemical Engineering Science, 65 (2010) 5495-5506.

[15] N.J. Divins, E. López, M. Roig, T. Trifonov, A. Rodríguez, F.G.d. Rivera, L.I. Rodríguez, M. Seco, O. Rossell, J. Llorca, Chemical Engineering Journal, 167 (2011) 597-602.

[16] X. Ouyang, R.S. Besser, Journal of Power Sources, 141 (2005) 39-46.

[17] D.I. Potemkin, P.V. Snytnikov, V.D. Belyaev, V.A. Sobyanin, Chemical Engineering Journal, 176–177 (2011) 165-171.

[18] S. Cruz, O. Sanz, R. Poyato, O.H. Laguna, F.J. Echave, L.C. Almeida, M.A. Centeno, G. Arzamendi, L.M. Gandia, E.F. Souza-Aguiar, M. Montes, J.A. Odriozola, Chemical Engineering Journal, 167 (2011) 634-642.

[19] O.H. Laguna, W.Y. Hernández, G. Arzamendi, L.M. Gandía, M.A. Centeno, J.A. Odriozola, Fuel, 118 (2014) 176-185.

[20] O.H. Laguna, E.M. Ngassa, S. Oraá, A. Álvarez, M.I. Domínguez, F. Romero-Sarria, G. Arzamendi, L.M. Gandía, M.A. Centeno, J.A. Odriozola, Catalysis Today, 180 (2012) 105-110.

[21] G. Arzamendi, I. Uriz, P.M. Diéguez, O.H. Laguna, W.Y. Hernández, A. Álvarez, M.A. Centeno, J.A. Odriozola, M. Montes, L.M. Gandía, Chemical Engineering Journal, 167 (2011) 588-596.

[22] N. Bion, F. Epron, M. Moreno, F. Mariño, D. Duprez, Top. Catal., 51 (2008) 76-88.

[23] P.V. Snytnikov, D.I. Potemkin, E.V. Rebrov, V.A. Sobyanin, V. Hessel, J.C. Schouten, Chemical Engineering Journal, 160 (2010) 923-929.

[24] E.R. Delsman, B.J.P.F. Laarhoven, M.H.J.M. De Croon, G.J. Kramer, J.C. Schouten, Chemical Engineering Research and Design, 83 (2005) 1063-1075.

[25] P.V. Snytnikov, M.M. Popova, Y. Men, E.V. Rebrov, G. Kolb, V. Hessel, J.C. Schouten, V.A. Sobyanin, Applied Catalysis A: General, 350 (2008) 53-62.

[26] I. Uriz, G. Arzamendi, P.M. Diéguez, L.M. Gandía, Chapter 17 - Computational Fluid Dynamics as a Tool for Designing Hydrogen Energy Technologies, in: P.M. Diéguez, L.M. Gandía, G. Arzamendi (Eds.) Renewable Hydrogen Technologies, Elsevier, Amsterdam, 2013, pp. 401-435.

[27] G.W. Roberts, P. Chin, X. Sun, J.J. Spivey, Applied Catalysis B: Environmental, 46 (2003) 601-611.

[28] P.B. Weisz, J.S. Hicks, Chemical Engineering Science, 50 (1995) 3951-3958.

[29] L.C. Almeida, O. Sanz, D. Merino, G. Arzamendi, L.M. Gandía, M. Montes, Catalysis Today, 215 (2013) 103-111.

[30] http://www.webelements.com/compounds/.

Tables

Table 1. Feed-stream compositions for the different catalytic activity tests

Feed-Stream	CO vol.%	O_2 vol.%	H_2 vol.%	N_2 vol.%	CO_2 vol.%	H_2O vol.%	λ
A	1.0	1.0	50.0	48.0	--	--	2.0
B	2.0	1.0	50.0	47.0	--	--	1.0
C	2.0	1.5	50.0	46.5	--	--	1.5
D	2.0	3.0	50.0	45.0	--	--	3.0
E	1.0	1.0	50.0	46.0	2.0	--	2.0
F	1.0	1.0	50.0	38.0	--	10	2.0
G	1.0	1.0	50.0	36.0	2.0	10	2.0

Figure Captions

Figure 1. Manufacturing of the microreactor prototype: (a) Micromilled plates; (b) Joining of the plates; c) Final microchannels block

Figure 2. Catalytic activity of the three evaluated systems (CuO_x/CeO_2 powder, MR150 and MR300) in the PROX reaction: (A) CO conversion; B) Selectivity to CO oxidation

Figure 3. Catalytic activity of the microreactors (MR150 and MR300) modifying the space velocity: (A) CO conversion; (B) Selectivity to CO oxidation

Figure 4. Catalytic activity during the PROX reaction of MR150 and MR300 modifying the λ value in the feed-stream: (A) CO oxidation; (B) Selectivity to CO oxidation

Figure 5. Catalytic activity of the MR150 and MR300 including CO_2 and/or H_2O in the feed-stream: (A) CO oxidation; (B) Selectivity to CO oxidation

Figure 6. Effectiveness factor as a function of the temperature during the PROX reaction for the CuO_x/CeO_2 powder catalysts, MR150 and MR300

Figure 1

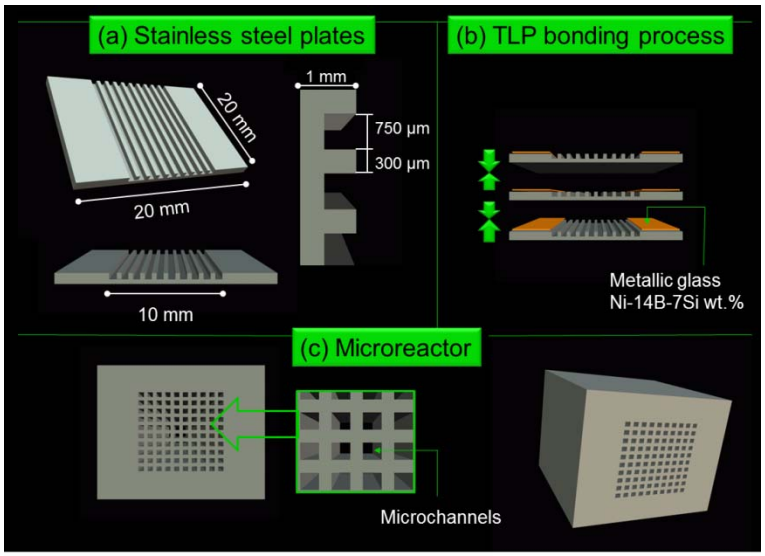
(a) Stainless steel plates
1 mm
20 mm
750 µm
300 µm
20 mm
10 mm
(b) TLP bonding process
Metallic glass
Ni-14B-7Si wt.%
(c) Microreactor
Microchannels

Figure 2

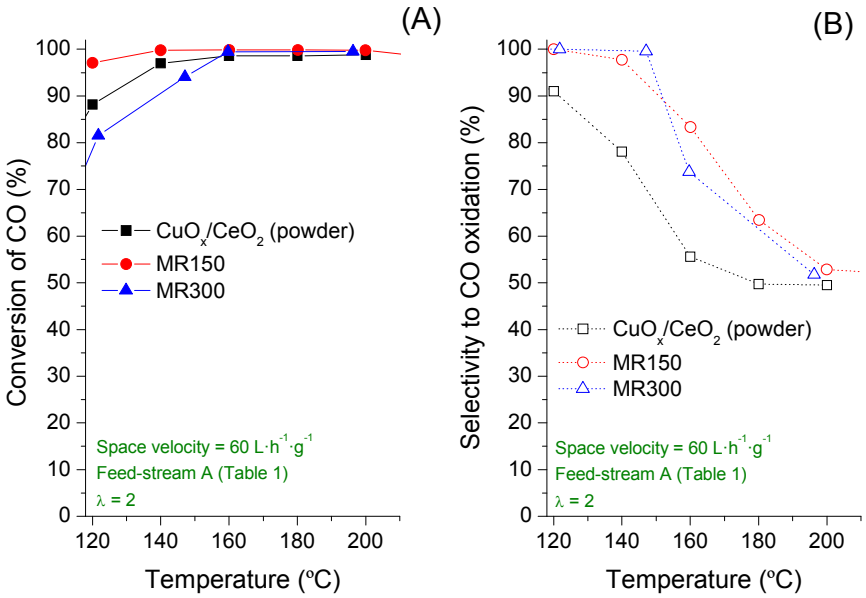
(A)
Conversion of CO (%)
Temperature (ºC)
CuOx/CeO2 (powder)
MR150
MR300
Space velocity = 60 L·h-1·g-1
Feed-stream A (Table 1)
λ = 2
(B)
Selectivity to CO oxidation (%)
Temperature (ºC)
CuOx/CeO2 (powder)
MR150
MR300
Space velocity = 60 L·h-1·g-1
Feed-stream A (Table 1)
λ = 2

Figure 3

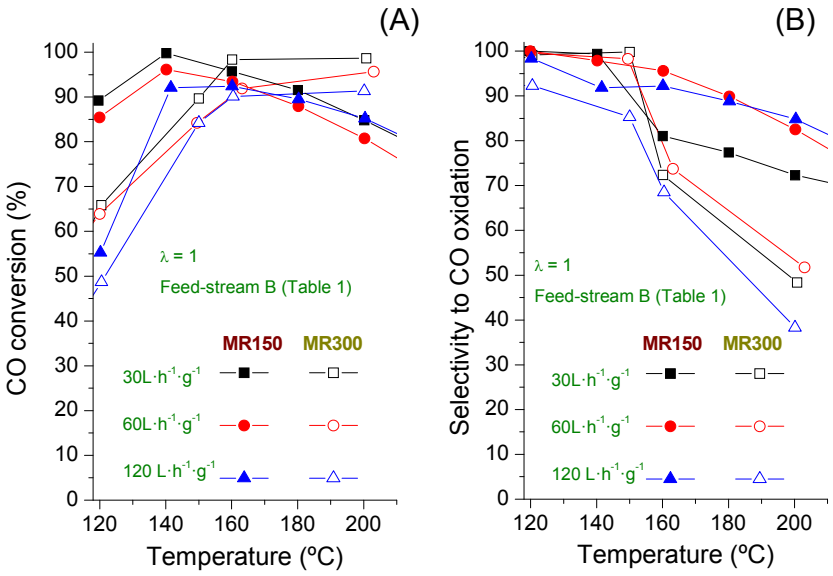
(A)
(B)
CO conversion (%)
Selectivity to CO oxidation
Temperature (ºC)
Temperature (ºC)
λ = 1
Feed-stream B (Table 1)
MR150
MR300
30L·h-1·g-1
60L·h-1·g-1
120 L·h-1·g-1

Figure 4

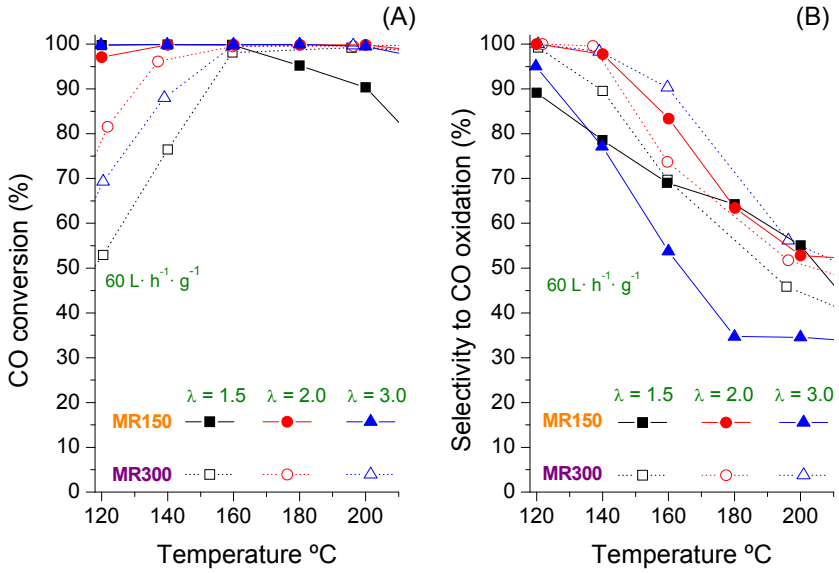
(A)
CO conversion (%)
Temperature ºC
60 L· h-1· g-1
λ = 1.5
λ = 2.0
λ = 3.0
MR150
MR300
(B)
Selectivity to CO oxidation (%)
Temperature ºC
60 L· h-1· g-1
λ = 1.5
λ = 2.0
λ = 3.0
MR150
MR300

Figure 5

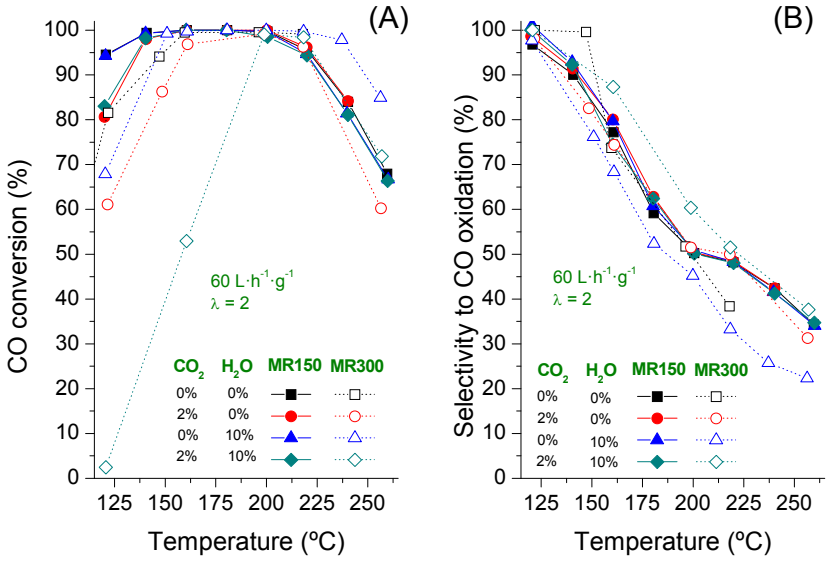
(A)
CO conversion (%)
Temperature (ºC)
60 L·h-1·g-1
λ = 2
CO2 H2O MR150 MR300
0% 0%
2% 0%
0% 10%
2% 10%
(B)
Selectivity to CO oxidation (%)
Temperature (ºC)
60 L·h-1·g-1
λ = 2
CO2 H2O MR150 MR300
0% 0%
2% 0%
0% 10%
2% 10%

Figure 6

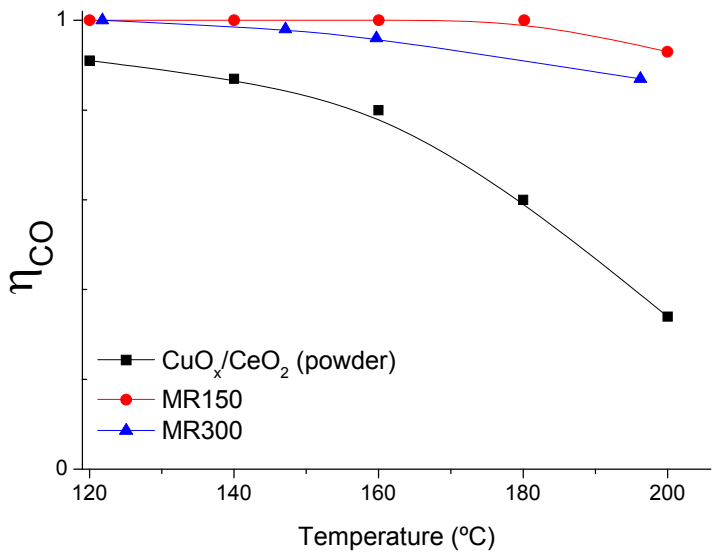
1
0
η_{CO}
120
140
160
180
200
Temperature (ºC)
CuO_x/CeO_2 (powder)
MR150
MR300